

## Discerning the Concentration and Bi-Directional Flux of Ammonia in an Urban Estuary Using the Relaxed Eddy Accumulation Method

Emily Joyce<sup>1,2</sup> , Sawyer Balint<sup>2</sup> , Wendell Walters<sup>1,2</sup> , Nebila Lichiheb<sup>3,4</sup> , Mark Heuer<sup>3,4</sup>, LaToya Myles<sup>3</sup> , Brian Heikes<sup>5</sup>, and Meredith Hastings<sup>1,2</sup> 

<sup>1</sup>Department of Earth, Environmental, and Planetary Sciences, Brown University, Providence, RI, USA, <sup>2</sup>Institute at Brown for Environment and Society, Brown University, Providence, RI, USA, <sup>3</sup>NOAA Air Resources Laboratory, Oak Ridge, TN, USA, <sup>4</sup>Oak Ridge Associated Universities, Oak Ridge, TN, USA, <sup>5</sup>Graduate School of Oceanography, University of Rhode Island, Narragansett, RI, USA

### Key Points:

- Dry deposition of gaseous ammonia and particulate ammonium comprises 9.6% of total nitrogen entering Narragansett Bay from the atmosphere
- The dominant flux of gaseous ammonia is upward (out of the water) during the fall season when surface water concentrations are elevated
- Ammonia released from Narragansett Bay to the atmosphere makes up to 10% of the local gaseous ammonia emission budget

### Supporting Information:

Supporting Information may be found in the online version of this article.

### Correspondence to:

E. Joyce,  
emily\_joyce@brown.edu

### Citation:

Joyce, E., Balint, S., Walters, W., Lichiheb, N., Heuer, M., Myles, L., et al. (2023). Discerning the concentration and bi-directional flux of ammonia in an urban estuary using the relaxed eddy accumulation method. *Journal of Geophysical Research: Biogeosciences*, 128, e2023JG007414. <https://doi.org/10.1029/2023JG007414>

Received 2 FEB 2023

Accepted 24 JUL 2023

### Author Contributions:

**Conceptualization:** Emily Joyce, Sawyer Balint, Wendell Walters, LaToya Myles, Brian Heikes, Meredith Hastings

**Data curation:** Emily Joyce, Sawyer Balint, Brian Heikes, Meredith Hastings

**Formal analysis:** Emily Joyce, Sawyer Balint, Wendell Walters, Brian Heikes, Meredith Hastings

**Funding acquisition:** Brian Heikes, Meredith Hastings

**Investigation:** Emily Joyce, Sawyer Balint, Brian Heikes, Meredith Hastings

**Methodology:** Emily Joyce, Sawyer Balint, Wendell Walters, Nebila Lichiheb, Mark Heuer, Brian Heikes, Meredith Hastings

**Project Administration:** Meredith Hastings

**Abstract** Narragansett Bay, the largest estuary in New England, is a heavily urbanized watershed impacted by deposition and runoff. Nutrient budgets and local policy rely on deposition data from a 1990 study that did not include any direct observations of dry deposition of gaseous ammonia ( $\text{NH}_{3(g)}$ ) and particulate ammonium ( $\text{p-NH}_4^+$ ) due to uncertainties in their flux direction and measurement difficulty. Recent work has shown that wet deposition of ammonium ( $\text{NH}_4^+$ ) to the Bay has increased by a factor of 6 over the past three decades, leading to a 2.5-fold increase in wet nitrogen (N) deposition. This documented increase in wet deposition of  $\text{NH}_4^+$  is concurrent with managed nutrient reductions in urbanized estuaries but has potentially increased the impacts of atmospheric N deposition, including the dry deposition of  $\text{NH}_{3(g)}$  and  $\text{p-NH}_4^+$ . However, the lack of  $\text{NH}_{3(g)}$  and  $\text{p-NH}_4^+$  measurements hinders our interpretation of this important N source. For the first time over Narragansett Bay, and to our knowledge over open water, dry (particulate and gas phase) total ammonia ( $\text{NH}_x = \text{NH}_{3(g)} + \text{p-NH}_4^+$ ) and the bidirectional  $\text{NH}_{3(g)}$  flux were quantified using a relaxed eddy accumulation sampling technique. We find that dry deposition of  $\text{NH}_x$  comprises 9.6% of total (wet + dry) N deposition. During the fall season, the dominant flux direction for  $\text{NH}_{3(g)}$  is upward, which also has implications for urban air quality. We estimate that  $\text{NH}_{3(g)}$  emitted from the Bay to the atmosphere makes up to 10% of the local  $\text{NH}_{3(g)}$  emission budget for fall.

**Plain Language Summary** Estuaries around the world receive nitrogen from various sources, including from the atmosphere through rainfall (wet deposition) and gasses and particulates (dry deposition). Such is the case in Narragansett Bay, RI, where a scarcity of measurements hinders our understanding of how atmospheric nitrogen influences this system. Recent work has shown that wet deposition has increased by 2.5-fold since 1990, driven by a 6-fold increase in ammonium wet deposition. Gaseous ammonia is subjected to few emission regulations and is poorly understood because gaseous ammonia can flux upward and downward (bi-directional). For the first time over Narragansett Bay, and to our knowledge over open water, dry deposition of total ammonia (gaseous ammonia + particulate ammonium) and the gaseous ammonia flux were quantified using a technique called relaxed eddy accumulation. We found that dry deposition of total ammonia made up 9.6% of total nitrogen deposition. The dominant flux direction of gaseous ammonia was upward (i.e., out of the water) during the fall season. Loss of nitrogen from the Bay to the atmosphere has implications for urban air quality. We estimated that gaseous ammonia emitted from the Bay to the atmosphere makes up to 10% of the local gaseous ammonia emission budget.

## 1. Motivation and Background

Anthropogenic changes to nutrient cycling have had a profound impact in estuaries, where excess nitrogen (N) fuels primary production and subsequent degradation in water quality (i.e., eutrophication) (Bricker et al., 2008). Efforts to combat eutrophication in estuaries have identified the need to reduce N loading from wastewater, agricultural runoff, and other anthropogenic sources, but these efforts have been complicated by the uncertain magnitude and temporal-spatial variability of additional sources and sinks of N, such as atmospheric deposition. N loading from the atmosphere has been observed to increase phytoplankton productivity in several systems (Aguilar et al., 1999; Balint et al., 2021; Knap et al., 1986; Paerl, 1995). As managed nutrient reductions begin

**Resources:** Emily Joyce, Sawyer Balint, Mark Heuer, LaToya Myles, Brian Heikes, Meredith Hastings

**Software:** Emily Joyce, Sawyer Balint, Brian Heikes, Meredith Hastings

**Supervision:** Emily Joyce, Brian Heikes, Meredith Hastings

**Validation:** Nebila Lichiheb, Mark Heuer, LaToya Myles, Brian Heikes, Meredith Hastings

**Visualization:** Emily Joyce, Sawyer Balint, Brian Heikes, Meredith Hastings

**Writing – original draft:** Emily Joyce, Sawyer Balint, Brian Heikes, Meredith Hastings

**Writing – review & editing:** Emily Joyce, Sawyer Balint, Wendell Walters, Nebila Lichiheb, LaToya Myles, Brian Heikes, Meredith Hastings

to take effect in urbanized estuaries, the relative importance of atmospheric deposition may increase (Decina et al., 2017; Loughner et al., 2016; Rao et al., 2014; Redling et al., 2013). Observations in Boston, MA and recent modeling studies in the Chesapeake Bay region suggest that atmospheric deposition is underestimated in urban systems by as much as a factor of 5 on an annual basis (Loughner et al., 2016; Rao et al., 2014).

Much of our understanding of atmospheric N deposition comes from the impressive array of National Atmospheric Deposition Program (NADP), Clean Air Status and Trends Network (CASNET), and Ammonia Monitoring Network (AMoN) monitoring sites across the USA. Inorganic N (nitrate ( $\text{NO}_3^-$ ) and ammonium ( $\text{NH}_4^+$ )) can enter estuaries from the atmosphere through wet (i.e., precipitation) or dry (i.e., gasses and aerosol) deposition. Comparatively, the total (wet + dry) amount of N deposited in the Eastern USA has been higher than in the Western USA (Benish et al., 2022).  $\text{NH}_4^+$  concentrations in wet deposition have increased at 90% of USA monitoring sites from 1985 to 2002 (Lehmann et al., 2005). In parallel, as N oxides ( $\text{NO}_x = \text{NO} + \text{NO}_2$ ) emissions (precursor to  $\text{NO}_3^-$  deposition) in the USA continue to decrease due to regulations (e.g., the Clean Air Act), ammonia ( $\text{NH}_{3(g)}$ ) emissions (precursor to  $\text{NH}_4^+$  deposition) remain relatively unregulated. Wet deposition of  $\text{NH}_4^+$  is predicted to now constitute between 37% and 83% of wet inorganic N deposition in the USA (Davidson et al., 2011; Fenn et al., 2018). Moreover, reductions in  $\text{NO}_x$ , as well as sulfur dioxide ( $\text{SO}_2$ ), have decreased the amount of partitioning to the particle phase (i.e., p- $\text{NH}_4^+$ ), and thus increased the amount remaining in the gas phase ( $\text{NH}_{3(g)}$ ) (Requia et al., 2019; Van Damme et al., 2020; Vannucci & Cohen, 2022). Given the short depositional lifetime of  $\text{NH}_{3(g)}$  (0.5 hr–0.46 days, as opposed to 3.2 days for p- $\text{NH}_4^+$ ; Xu & Penner, 2012), the shift toward the gaseous phase has important implications for depositional patterns. It is likely that  $\text{NH}_{3(g)}$  is removed close to its emission source, especially if it has reached cloud level, because precipitation efficiently scavenges  $\text{NH}_{3(g)}$  (Asman et al., 1998; Fowler et al., 1997; Xu & Penner, 2012).  $\text{NH}_{3(g)}$  is the primary alkaline molecule in the atmosphere and plays a key role in numerous atmospheric and climatic processes (Asman et al., 1998; Seinfeld & Pandis, 1979). The wet and dry deposition of  $\text{NH}_4^+$  species represents a bioavailable source of reactive N, and a potential ingredient for the degradation of waters and soils (Betz & Groffman, 2013; Galloway et al., 2004; Howarth, 2008; Knap et al., 1986; Michaels et al., 1993).

Narragansett Bay, RI, USA epitomizes the complexity of investigating atmospheric N deposition in the context of managed N reductions in an urbanized estuary. Although contemporary N budgets assume that wet and dry atmospheric deposition in this system have remained unchanged since they were measured in 1988–1990 (Fraher, 1991; Narragansett Bay Estuary Program, 2017; Nixon et al., 1995; Schmidt, 2014), recent works suggest that Narragansett Bay, like much of the nation, has experienced large increases in atmospheric N deposition due to increases in wet deposition of  $\text{NH}_4^+$ . Event-based precipitation collected in Providence, RI found that total inorganic N directly entering the Bay via wet deposition is currently underestimated by at least a factor of ~2.5 times (Joyce et al., 2020) due to a ~6-fold increase in  $\text{NH}_4^+$  deposition. Although there are large uncertainties regarding the role of atmospheric N in Narragansett Bay N cycling, recent work shows that precipitation-derived sources of N (e.g., stormwater runoff) constitute a large component of the N budget (Balint et al., 2021). Scaling recent precipitation-derived N observations using the Nixon et al. (1995) framework, which is used in policy today, yields a total of  $1,179 \times 10^3 \text{ kg N yr}^{-1}$  (Balint et al., 2021) compared to the currently used estimate of  $419 \times 10^3 \text{ kg N yr}^{-1}$  (Narragansett Bay Estuary Program, 2017; Nixon et al., 1995). Dry deposition is typically modeled to represent an additional 40%, but the bi-directional exchange capability of  $\text{NH}_{3(g)}$  makes its exact magnitude uncertain (Bash et al., 2013). In fact,  $\text{NH}_{3(g)}$  in previous dry deposition estimates has not been included due to uncertainties in the flux direction (Fraher, 1991). Dry deposition not only represents an important and under-constrained component of direct deposition to the Bay, but also has an indirect role through stormwater runoff.

Given the vast increase in wet deposition of  $\text{NH}_4^+$  in the recent past and the significant uncertainty underlying dry deposition estimates, there is a critical need to quantify atmospheric deposition of total ammonia ( $\text{NH}_x = \text{NH}_{3(g)} + \text{p-NH}_4^+$ ) to Narragansett Bay. For the first time, dry (particulate and gas phase) deposition of  $\text{NH}_x$  and the bi-directional  $\text{NH}_{3(g)}$  flux were quantified over Narragansett Bay using a relaxed eddy accumulation (REA) sampling technique (Fotiadi et al., 2005). To our knowledge, this is also the first attempt at deploying the REA system over open water. This method requires precise knowledge of local micrometeorology and a method for separately collecting  $\text{NH}_{3(g)}$  (gas phase) and p- $\text{NH}_4^+$  (particle phase) (Meyers et al., 2006; Nelson et al., 2017). The REA methodology has demonstrated the ability to quantify  $\text{NH}_3$  flux measurements in agricultural (Nelson et al., 2017) and salt marsh studies (Lichiheb et al., 2021), and thus may be an appropriate approach for dry

deposition measurements over Narragansett Bay. Here, we test this approach by deploying the system in Narragansett Bay to inform our understanding of N dynamics in this study system and other urbanized estuaries.

## 2. Methods and Approach

### 2.1. Study System

Narragansett Bay, RI, USA is a temperate estuary located within RI and MA with an extensive history of N pollution and contemporary mitigation efforts (Nixon et al., 2008; Oczkowski et al., 2018). There are north-south gradients in salinity, urbanization, and eutrophication, with the heavily urbanized Providence River Estuary at the head of the Bay experiencing the greatest N loading from wastewater treatment facilities, freshwater riverine loading, stormwater, and atmospheric deposition (NBEP, 2017). Dry deposition of  $\text{NH}_x$  directly to the Bay was determined using a REA sampling technique in October 2019 and in September–October 2020. The REA sampling system was erected at  $41^\circ47'23.32''\text{N}$ ,  $71^\circ22'25.36''\text{W}$ , placing it 1.2 km southeast of Fields Point wastewater treatment facility, 3.6 km south of Interstate 195, and amidst the densely urbanized City of Providence two of its adjacent suburbs, Cranston and East Providence (Figure 1).

The predominant wind direction during the summer and fall is from the south, and the location was selected to provide overwater fetch that was  $>0.5$  km and which extended from due south westward to the north-northwest. The REA sampling system was mounted on a fixed piling 40 m from shore and was accessible via a floating dock.

### 2.2. Relaxed Eddy Accumulation and Eddy Covariance Flux Methods

The vertical flux of  $\text{NH}_{3(\text{g})}$  was estimated using the relaxed eddy-accumulation method, REA, (Businger & Oncley, 1990), as implemented by Meyers et al. (2006). The system is composed of an ultrasonic anemometer (RM Young, Model: 81000VRE) interfaced with solenoid valves (WIC Valve, Model: 2ACK-1/4) and a mass flow controller (Aalborg, Model: GFCS-018856) via a computer (Figure 2). The mass flow controller was calibrated at the University of Rhode Island at Temperature =  $25^\circ\text{C}$ , Pressure = 1 atm. Three separate filter pack trains (described below) were used to sample updraft, downdraft, and deadband (i.e.,  $\pm 0.11$  m  $\text{s}^{-1}$ ) periods (Nelson et al., 2017). During operation, the vertical velocity of the ambient air, as detected from the anemometer, was used to determine whether the instrument was operating in an updraft, downdraft, or deadband condition at 1 Hz resolution (Meyers et al., 2006). The solenoid valves were operated to select the appropriate filter train, and air was drawn through them at  $16.7$  L  $\text{min}^{-1}$  using a vacuum pump (Welch 2546B-01) A flow rate of  $16.7$  L  $\text{min}^{-1}$  was selected because it was the maximum flow rate that could be used for  $\text{NH}_{3(\text{g})}$  and  $\text{p-NH}_4^+$  collection with the filter packs. A fourth filter pack train served as a field blank. Average air temperature, wind speed, and wind direction were recorded from the anemometer at a 30-min time resolution. The REA sampling system was mounted on a 3 m aluminum tower fixed to a wooden piling, accessible from a floating dock.

The flux of  $\text{NH}_{3(\text{g})}$  as calculated by the REA system is algebraically expressed by:

$$F_{\text{REA}}(\text{NH}_{3(\text{g})}) = \beta \sigma_w \left( \overline{[\text{NH}_{3(\text{g})}]^\uparrow} - \overline{[\text{NH}_{3(\text{g})}]^\downarrow} \right) \quad (1)$$

where,  $F_{\text{REA}}(\text{NH}_{3(\text{g})})$  is the REA-determined flux of  $\text{NH}_{3(\text{g})}$ ,  $\sigma_w$  is the standard deviation of the vertical velocity,  $\overline{[\text{NH}_{3(\text{g})}]^\uparrow}$  is the mean concentration of  $\text{NH}_{3(\text{g})}$  in updrafts,  $\overline{[\text{NH}_{3(\text{g})}]^\downarrow}$  is the mean concentration of  $\text{NH}_{3(\text{g})}$  in the downdrafts, and  $\beta$  is an empirical proportionally coefficient. The 1-s average vertical wind component is used to trigger the valves, which permit the collection of updraft and downdraft samples and determine  $\overline{[\text{NH}_{3(\text{g})}]^\uparrow}$  and  $\overline{[\text{NH}_{3(\text{g})}]^\downarrow}$ . The coefficient  $\beta$  is estimated from the sensible heat fluxes determined using: (a) the REA method applied to temperature, and (b) the sensible heat flux determined using an eddy-covariance (EC; Equation 2) measurement. The two fluxes are measured by the sonic anemometer used in the REA– $\text{NH}_{3(\text{g})}$  method to control the valve switching and to determine the vertical velocity variance. The vertical velocity measurement is used to sift and average  $T$  in updrafts and downdrafts,  $\overline{[T]^\uparrow}$  and  $\overline{[T]^\downarrow}$ . The EC sensible heat flux method is algebraically expressed by:

$$F_{\text{EC}}(T) = \overline{w'T'} \quad (2)$$

where,  $F_{\text{EC}}(T)$  is the vertical flux of sensible heat,  $w'$  is the vertical velocity perturbation,  $T'$  is the perturbation in  $T$ , and  $\overline{w'T'}$  is the time-averaged product of the vertical velocity perturbation and temperature perturbation. The

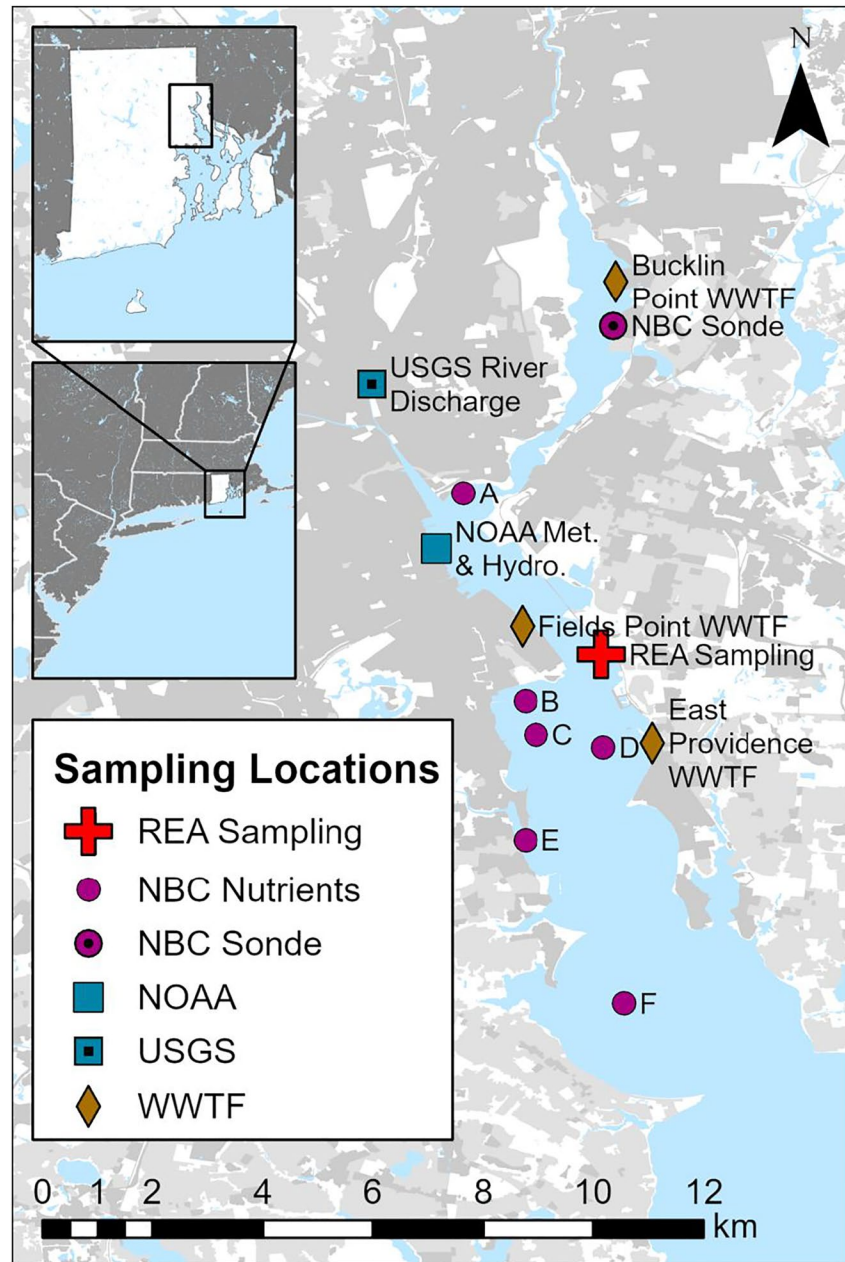


**Figure 1.** Map of Providence River Estuary displaying the dry deposition sampling (relaxed eddy accumulation (REA)), water quality sampling (Narragansett Bay Commission (NBC, 2021a) buoys and sonde), and meteorological (National Oceanic and Atmospheric Administration (NOAA)) and river discharge (United States Geological Survey (USGS)) station locations utilized in this study and their relation to N point sources (i.e., wastewater treatment facility (WWTF)). Urbanization is displayed by gray scale, with the darkest gray color representing the highest level of urbanization (RIGIS, 2022).

EC sample averaging time used to calculate  $\beta$  for the  $\text{NH}_{3(g)}$  flux was equal to the  $\text{NH}_3$  filter pack sample interval, normally 4 hr.  $\beta$  is the ratio of the REA flux to the EC flux:

$$\beta = \frac{F_{\text{REA}}(T)}{F_{\text{EC}}(T)} = \frac{\langle w'T' \rangle}{\sigma_w(T^\uparrow - T^\downarrow)} \quad (3)$$

The scalar flux of heat is assumed to capture the same dynamical flux processes as that for a chemical scalar flux and  $\beta$  for the sensible heat flux can therefore be used to estimate  $\beta$  for the  $\text{NH}_{3(g)}$  flux. An implicit assumption

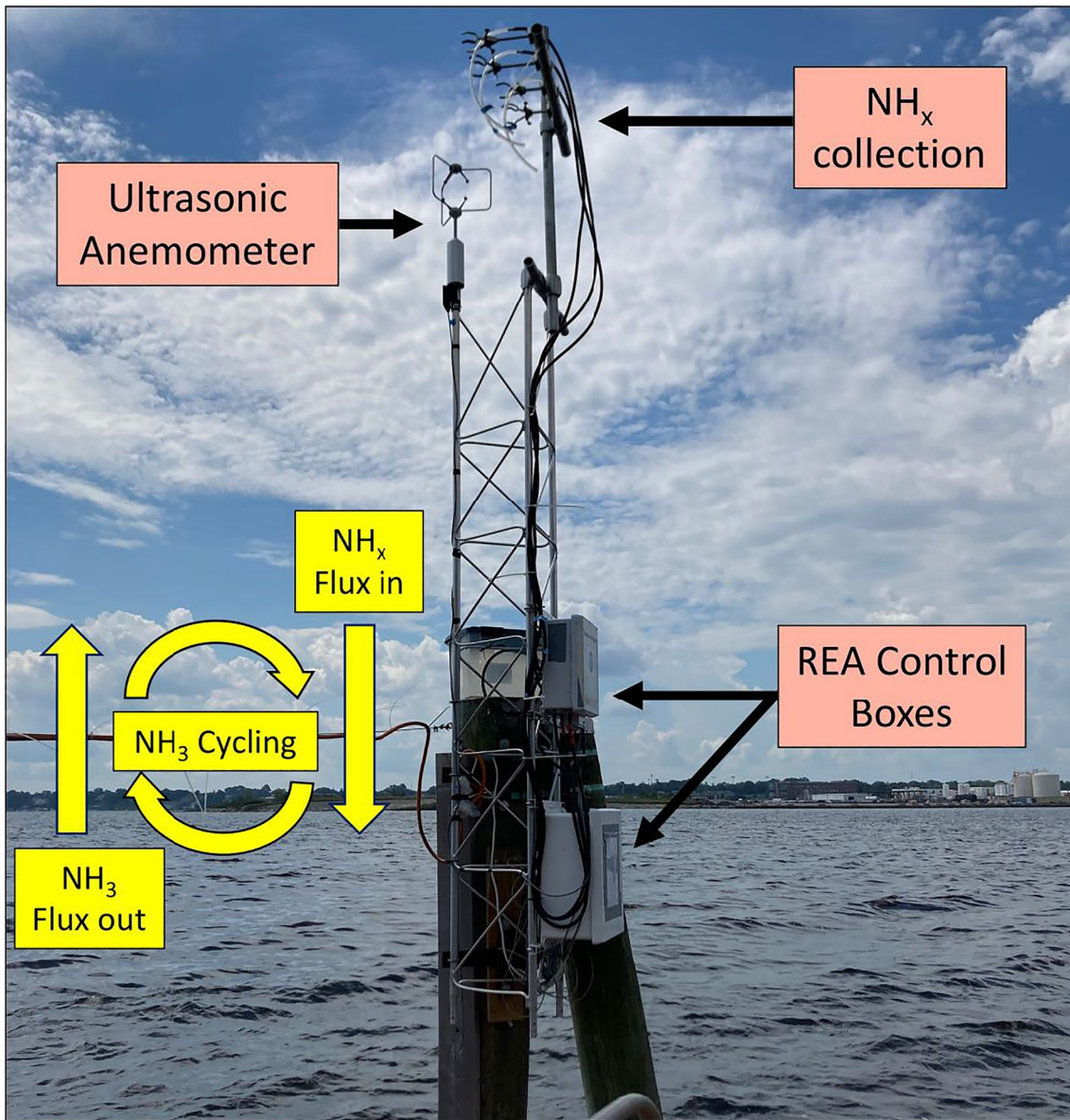


**Figure 2.** Dry deposition collection of total ammonia ( $\text{NH}_x = \text{NH}_{3(g)} + \text{p-NH}_4^+$ ). The REA control boxes, which control sample collection, are attached to a 3 m tower. Samplers are connected to the tubing positioned on top of the tower, which sit at the same height as the anemometer. A vacuum pump is housed within a plastic box on top of the piling. This sampling set up allows for direct  $\text{NH}_{3(g)}$  flux measurement (i.e.,  $\text{NH}_{3(g)}$  into and out of the water).

in the above determination of  $\beta$  is that both sensible heat flux estimates share a common mean air density and specific heat capacity such that these terms cancel when the two fluxes are ratioed in (Equation 3) and therefore were not included in (Equation 1) and (Equation 2).

LI-COR EddyPro 7.0 software (Fratini & Mauder, 2014; LI-COR Biosciences, 2021) is used for EC quality control and to estimate 1-dimensional (1-D) upwind footprints of flux contribution using the method of Kljun et al. (2004). The EC sample averaging time is 30 min. A 1-D footprint is aligned with the 30-min wind direction. The sample site is taken as the origin and distance increases radially into the wind. The 1-D footprint estimates the cumulative fraction of the flux between the measurement site and the upwind distance. The fetch distance accounts for 10% and 90% of the sensible heat flux for a given wind direction. Figure 3 displays the 10th and 90th percentiles of the 1-D footprint for all recorded 30-min EC sampling periods as a function of wind direction.

Sample timing and duration (4 hr) depended on the REA and EC quality assurance process and the chemical analytical precision (Fotiadi et al., 2005; Jarvi, 2009). Samples were collected within 2 hr of high tide to minimize

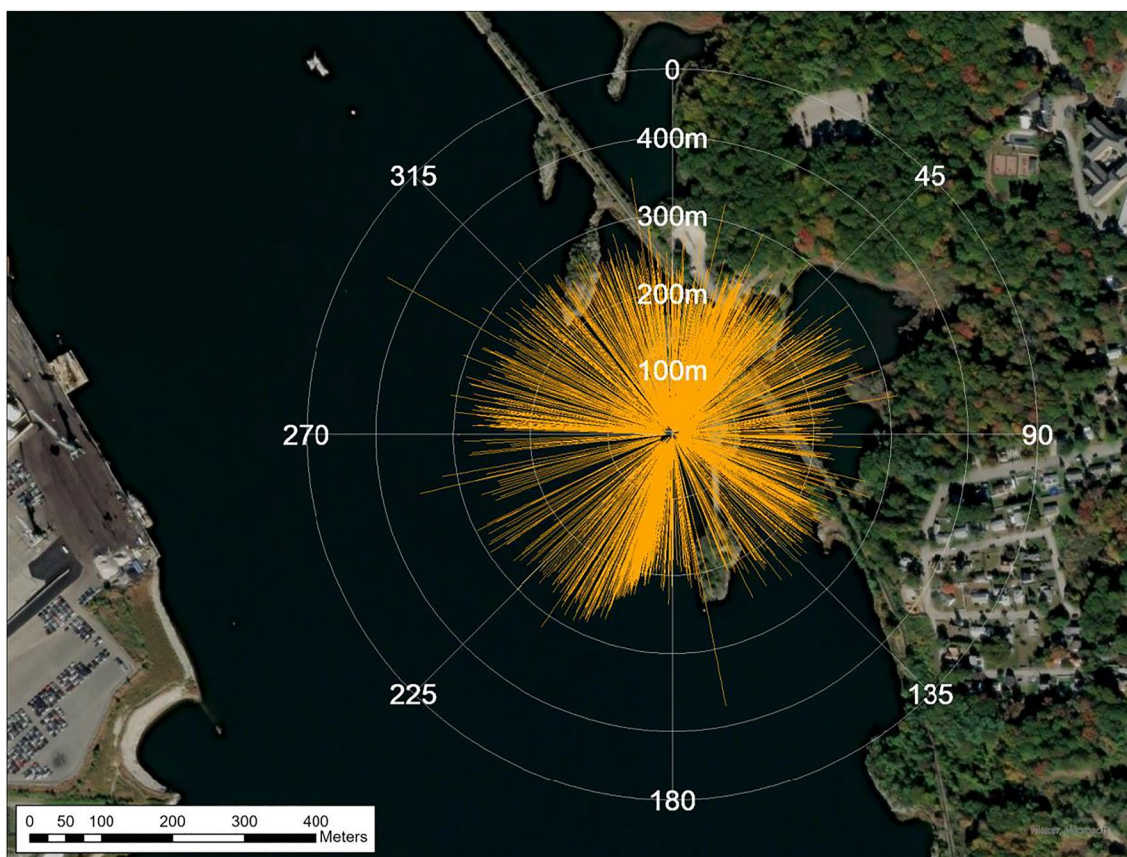


**Figure 3.** Cumulative flux contribution 1-D footprint as a function of 30 min mean wind direction. The minimum and maximum values of the orange segment represent the 10th and 90th percentiles, respectively, of the 1-D footprint from the flux measurement site.

dock height fluctuations. On average, the tide changed  $1.4 \pm 0.2$  m from high to low tide during the sampling period. Lastly, samples were not collected on days with precipitation to ensure that gasses and particles were not wet scavenged from the air column (preliminary work has shown that the gasses and particle concentrations sampled on rainy days were below our limit of detection), or on days with excessive wave height that prevented safe access to the system from the floating dock.

### 2.3. $\text{NH}_x$ Concentration Determination

Collection of particulate ammonium ( $\text{p-NH}_4^+$ ) and gaseous ammonia ( $\text{NH}_{3(\text{g})}$ ) was conducted using an open face inlet filter pack series, with a Teflon filter followed by a glass fiber filter coated in a 5% acid solution. Potential loss of  $\text{p-NH}_4^+$  was minimized using the open face inlet. Citric acid, oxalic acid, and phosphoric acid were each tested as potential solutions to use for collection. Citric acid exhibited the lowest  $\text{NH}_{3(\text{g})}$  blank and was therefore used for all sampling. A laboratory blank was collected before each sampling period, and a travel blank was collected every 3<sup>rd</sup> trip. Preparation and extraction of filters followed the NADP standard operating procedure (PR-4074; NADP, 2012). All filter samples were sonicated for 1-hr, filtered using a  $0.22 \mu\text{m}$  syringe filter, and frozen at  $-20^\circ\text{C}$  until subsequent analysis.  $\text{NH}_{3(\text{g})}$  and  $\text{p-NH}_4^+$  concentrations for each filter pack sample set (i.e., updraft, downdraft, deadband, laboratory blank, and field blank) were determined via a colorimetric method (SMARTCHEM EPA Compliant Method 350.1) using a discrete UV-Vis analyzer (Westco SmartChem 200). The limit of detection for  $[\text{NH}_4^+]$  was  $0.7 \mu\text{mol L}^{-1}$ . Based on repeated measures of standards, sample duplicates, and an in-house quality control sample, the pooled standard deviation ( $1\sigma$ ) for  $[\text{NH}_4^+]$  was  $0.6 \mu\text{mol L}^{-1}$ . Liquid concentrations ( $\mu\text{mol L}^{-1}$ ) were converted to air concentrations ( $\mu\text{g m}^{-3}$ ) based on extraction volume (L), run time (min), and volume of air sampled ( $\text{L min}^{-1}$ ). All laboratory and field blanks had detectable  $\text{NH}_x$  concentrations lower than the field samples, and thus were subtracted from field samples to determine final

concentrations. Ambient  $\text{NH}_x$  concentrations during the sampling runs were then calculated by summing  $\text{NH}_{3(g)}$  and  $\text{p-NH}_4^+$  concentrations. Finally,  $\text{NH}_{3(g)}$  fluxes for each sampling run were calculated using Equations 1–3.

#### 2.4. Local Environmental Measurements and Statistical Interpretation

Publicly available bi-weekly  $\text{NH}_{3(g)}$  surface water concentrations collected at six stations within the Providence River Estuary were obtained from the Narragansett Bay Commission (NBC, 2021a) for 2015–2020 (NBC, 2021a). These sites were chosen to capture any potential surface water nutrient concentration gradients. NBC station locations relative to the REA sample site are shown on Figure 1. Five years of data were compared to ensure the surface water concentrations observed during the REA sampling period were typical to prior years (Table S1 in Supporting Information S1). Water concentrations measured during the sampling dates in 2019 and 2020 were then used to characterize  $\text{NH}_{3(g)}$  water-atmospheric exchange. The maximum  $\text{NH}_{3(g)}$  loss to the atmosphere from the water was estimated using  $\text{NH}_{3(g)}$  concentration in the surface water, Henry's Law Constant, exchange velocity, and the surface area of the Providence River Estuary. Surface area was calculated to be 13 km<sup>2</sup> using ArcGIS Pro (RIGIS, 2022).

Six-minute resolution meteorological data (wind speed, wind direction, and air temperature) and physical oceanography data (water temperature, predicted tidal height, and observed tidal height) were obtained from the National Oceanic and Atmospheric Administration (NOAA) station 8454000 (wind speed, wind direction, air temperature, and water temperature data were not available for October 2019) (NOAA, 2020). Additionally, daily mean discharge data from the Providence River was obtained from the United States Geological Survey (USGS) station 01114000 (USGS, 2021). Finally, 15-min resolution water quality data (water temperature, pH, chlorophyll, and salinity) were obtained from NBC's Phillipsdale sonde, located upstream in the Seekonk River (NBC, 2019, 2020) (Table S2 in Supporting Information S1). Water quality monitoring methodology and data quality assurance are detailed in NBC 2021b. The average wind direction during each sampling event was used to assess the possibility of land interference. Data were binned as land, water, or indeterminate based on their 1-D footprint, as described above. Mean values of environmental observations taken during each REA sampling event were compared to  $\text{NH}_{3(g)}$  flux and concentration using a Pearson's linear correlation matrix. Differences in runtime between the updraft, downdraft, and deadband filter trains were assessed using an ANOVA with Tukey's HSD post-hoc testing after normality was confirmed with Shapiro-Wilks tests, while differences in  $\text{NH}_x$  concentration between directions were assessed using Kruskal-Wallis testing with Dunns post-hoc testing due to non-normality. Differences in  $\text{NH}_3$  surface water concentrations between years, seasons, and stations were assessed using Kruskal-Wallis testing with Dunns post-hoc testing due to non-normality. Analyses were performed in R version 4.2.1 (R Core Team, 2022).

### 3. Results

#### 3.1. REA Performance and $\text{NH}_3$ Flux

A total of 23 sampling periods were conducted, with 3 measurements in 2019 (October 19th to 20th) and 20 measurements in 2020 (August 26th to October 10th). Differences in runtime and concentration between the downdraft and updraft were not significant ( $p > 0.05$ ,  $n = 23$ ) (Figure S1 in Supporting Information S1). Air temperatures during sample collection ranged from 9.3 to 26.4°C and wind speeds ranged from 0.7 to 5.4 m/s<sup>2</sup>. Concentrations are reported as averages  $\pm$  one standard deviation ( $\pm 1\sigma$ ,  $n = 22$ ). Laboratory blanks were  $5.5 \pm 2.1 \mu\text{mol L}^{-1}$  and field blanks were  $6.7 \pm 2.1 \mu\text{mol L}^{-1}$ .  $\text{NH}_x$  concentrations (before blank corrections) were  $12.7 \pm 3.9 \mu\text{mol L}^{-1}$  for updraft;  $13.0 \pm 5.0 \mu\text{mol L}^{-1}$  for downdraft; and  $13.9 \pm 7.4 \mu\text{mol L}^{-1}$  for deadband. Thus,  $\text{NH}_x$  concentrations were low enough that blank  $\text{NH}_x$  originating from the coating solution, filter preparation, and/or transport to the sampling location constituted an average of 46% (range of 7.2%–92.5%) of the measured  $\text{NH}_x$ . After correcting for the blanks and converting to air concentrations, total  $\text{NH}_x$  ranged from 0.3 to 8.2  $\mu\text{g-N m}^{-3}$  (average  $2.1 \pm 1.8 \mu\text{g-N m}^{-3}$ ) for  $\text{NH}_{3(g)}$  and 0.0–0.2  $\mu\text{g-N m}^{-3}$  (average  $0.1 \pm 0.05 \mu\text{g-N m}^{-3}$ ) for  $\text{p-NH}_4^+$  (Figure 5; Table S3 in Supporting Information S1). (Please note that these values reflect the sum of updraft, downdraft, and deadband positions). The majority of dry  $\text{NH}_x$  was observed in the gas phase, which is similar to recent Providence, RI measurements during summer/fall conditions (Walters et al., 2022). By direction,  $\text{NH}_x$  concentrations across all events averaged  $0.6 \pm 0.4 \mu\text{g-N m}^{-3}$  for updraft;  $0.8 \pm 0.9 \mu\text{g-N m}^{-3}$  for downdraft; and  $0.7 \pm 0.5 \mu\text{g-N m}^{-3}$  for deadband (Figure S2 in Supporting Information S1).

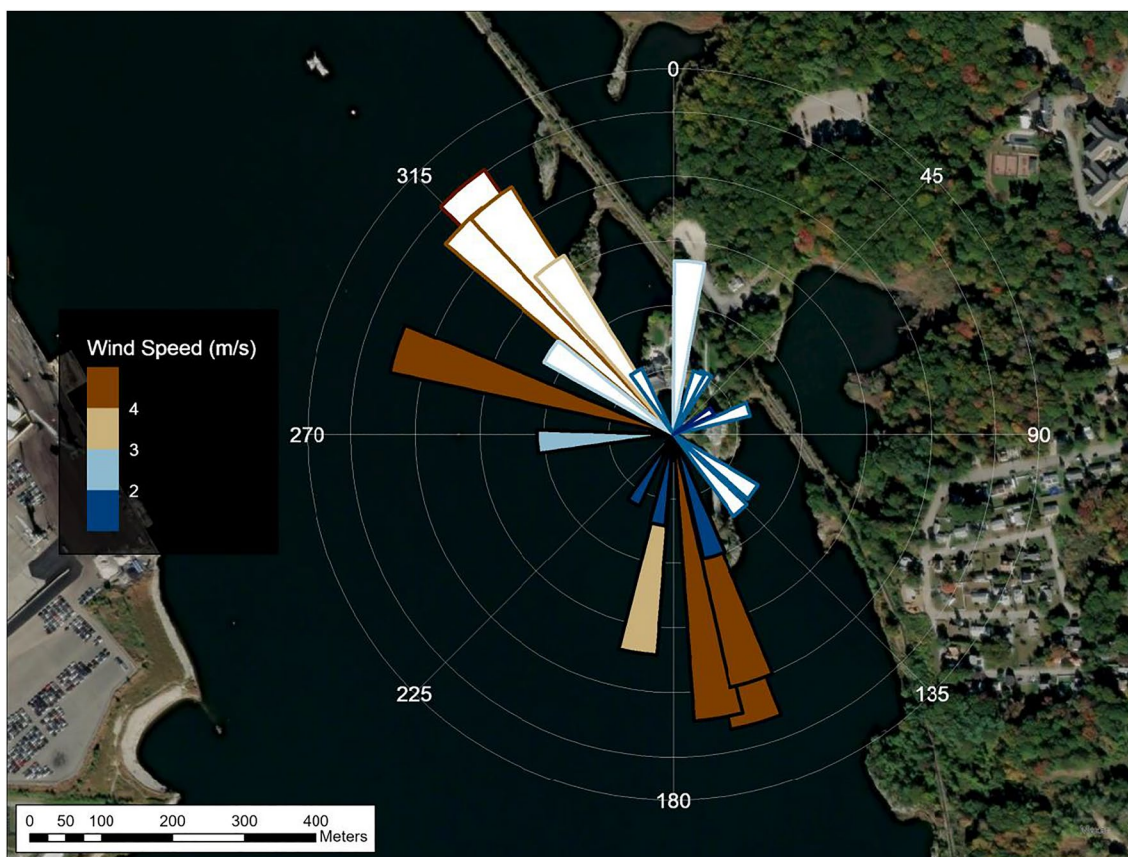


**Figure 4.** Satellite view of sample site overlaid by a wind rose displaying the fetch (outer circle), wind speed, and wind direction. Samples impacted by land influence are shown with white fill.

Eleven samples were influenced by land-to-sea air flow, hereafter referred to as “land-derived,” and were therefore removed for flux determination and analysis (Figure 4). Three samples were classified as “indeterminate” based on the possibility of land influence, and therefore were excluded from analysis. Because land interference was not certain, a flux for each indeterminate sample is reported in the Supporting Information S1. Fluxes are reported as positive for net volatilization (upward direction) and negative for net deposition (downward direction). The vertical flux of  $\text{NH}_{3(g)}$  was estimated for each sample where flow originated over the sea, hereafter referred to as “water-derived” ( $n = 9$ ; Figure 5). The net flux was close to zero, ranging from  $-2.3 \times 10^{-2}$  to  $6.8 \times 10^{-2} \mu\text{g-N m}^{-2} \text{s}^{-1}$  (average  $1.2 \times 10^{-2} \pm 4.0 \times 10^{-2}$ ).

### 3.2. Environmental Parameters and Statistical Analysis

Of the 23 total sampling periods, 9 were classified as water-derived based on wind direction (Figure 4, Table S4 in Supporting Information S1). The results from the linear correlation matrix are shown in Figure S3 and Table S5 in Supporting Information S1.  $\text{NH}_{3(g)}$  concentration exhibited a significant linear relationship with chlorophyll concentration measured at the NBC sonde when land and water samples were considered ( $p = 0.032$ ,  $r^2 = 0.23$ ,  $n = 20$ ) and water-derived samples ( $p = 0.034$ ,  $r^2 = 0.50$ ,  $n = 9$ ) (Figure 6). Furthermore, a significant linear relationship was evident with pH for land and water samples ( $p = 0.034$ ,  $r^2 = 0.23$ ,  $n = 20$ ), but not for land or water samples considered individually (Figure 6).

Bi-weekly  $\text{NH}_{3(g)}$  surface water concentrations during the REA sampling period averaged  $5.8 \pm 5.2 \mu\text{mol L}^{-1}$ . Fall surface water concentrations for 2020 were significantly different from fall surface water concentrations recorded in 2018 ( $p = 0.0012$ ,  $n = 65$ ) but were not significantly different from 2016, 2017, or 2019 ( $p > 0.05$ ,  $n = 147$ ). Station location did not influence fall water concentration during 2019 or 2020 ( $p = 0.23$ ,  $n = 61$ ). Surface water concentrations during the fall of 2019 and 2020 were significantly lower than during the winter ( $p < 0.0001$ ,  $n = 116$ ) (Figure S4 in Supporting Information S1).

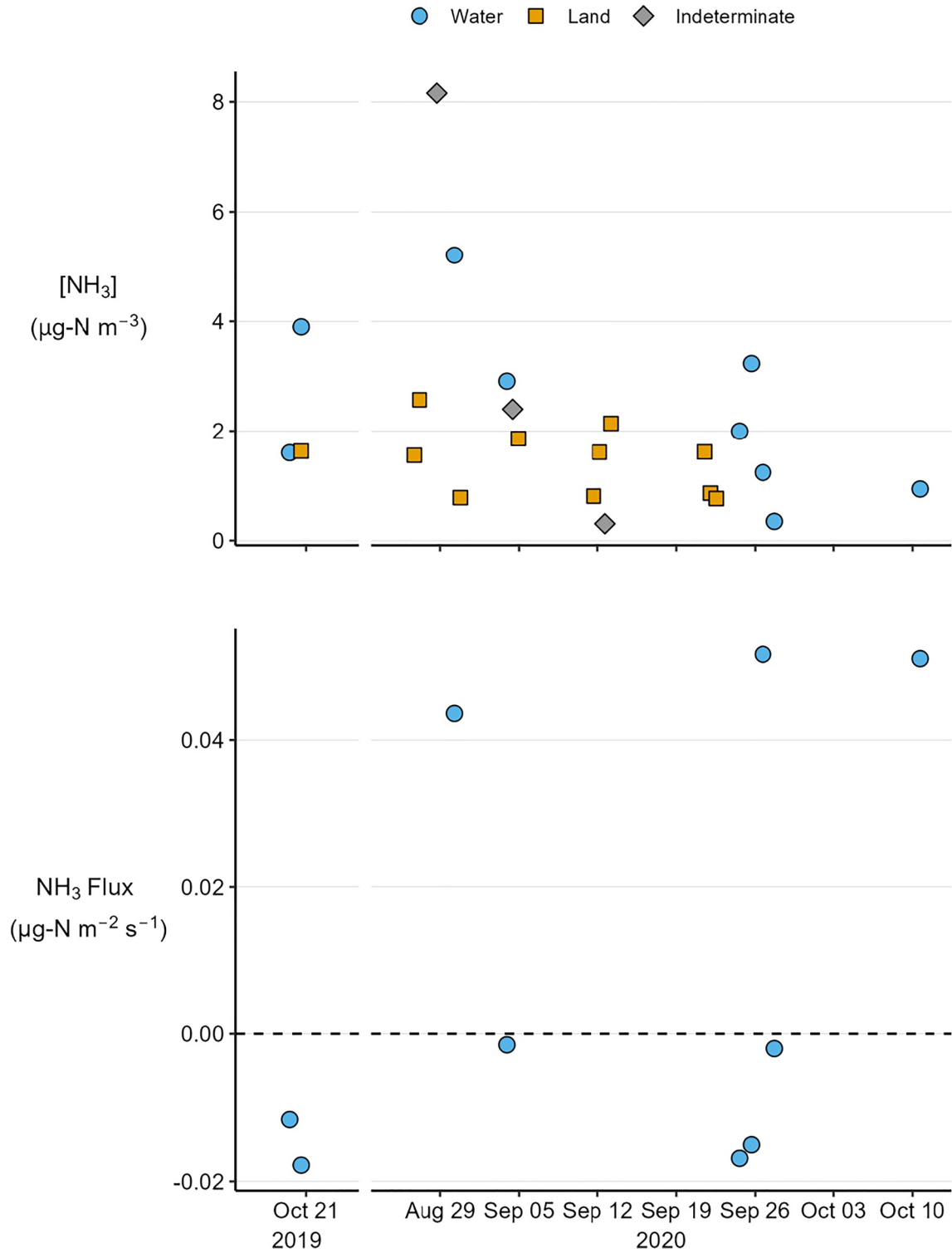


**Figure 5.** Times series displaying  $NH_{3(g)}$  concentration (top) and flux (bottom) versus sampling days.  $NH_{3(g)}$  concentrations are plotted by classification of water-derived, land-derived, and indeterminate (Table S4 in Supporting Information S1). A downward flux is displayed with a negative sign to represent the change in direction.

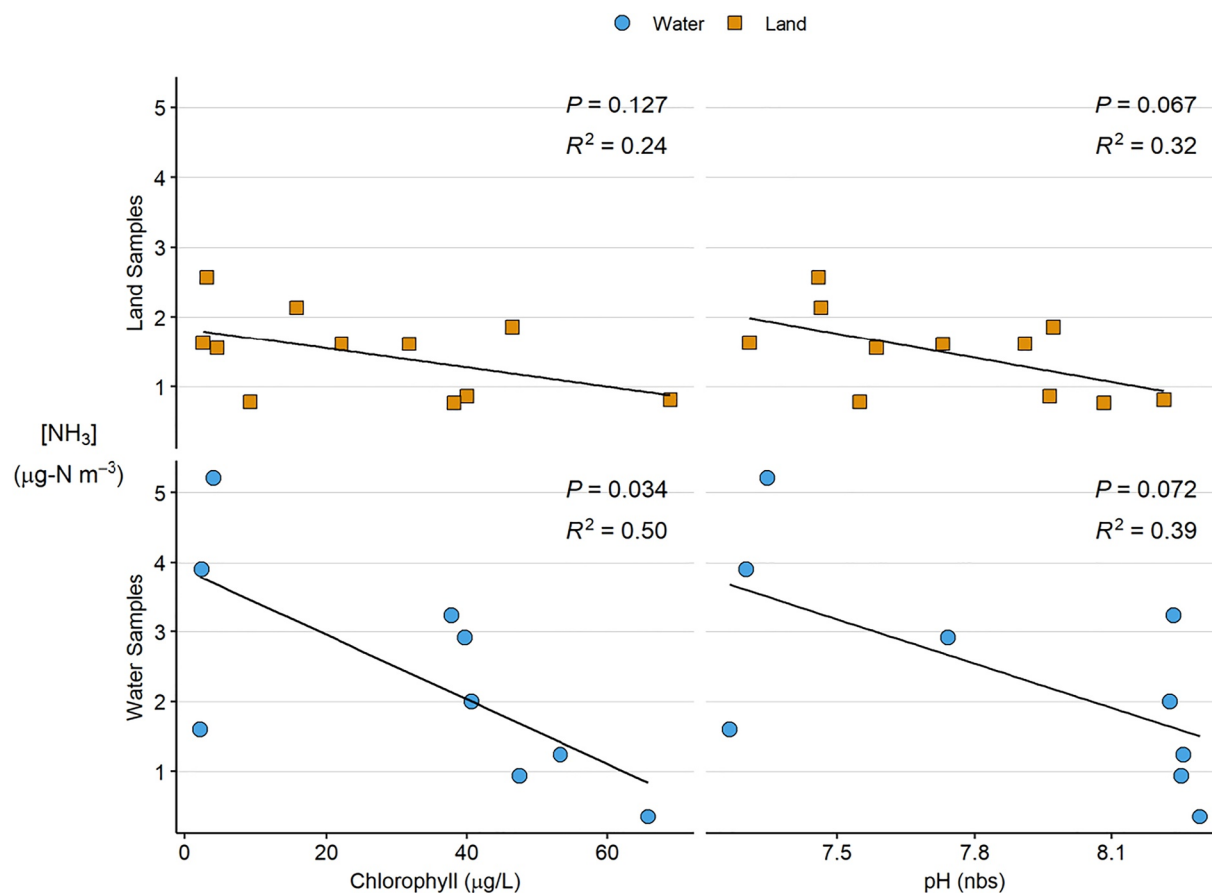


**Figure 6.** Linear regression between atmospheric NH<sub>3(g)</sub> concentration and surface water chlorophyll concentration (left) and surface water pH (right) for land-derived samples (top) and water-derived samples (bottom).

## 4. Discussion

### 4.1. NH<sub>x</sub> Concentration and NH<sub>3(g)</sub> Flux

Atmospheric NH<sub>3(g)</sub> concentrations observed in this study (0.3–8.2 μg-N m<sup>-3</sup>; average 2.1 ± 1.8 μg-N m<sup>-3</sup>) aligned with recent observations conducted over water (Table 1) and land. For example, NH<sub>3(g)</sub> above a grassland near Tampa, FL USA ranged from 1.3 to 8.7 μg-N m<sup>-3</sup> (average 3.5 ± 2.2 μg-N m<sup>-3</sup>; Myles et al., 2007), NH<sub>3(g)</sub> above a cornfield in Urbana, IL USA ranged from 0.3 to 8.1 μg-N m<sup>-3</sup> (average 2.6 ± 2.0 μg-N m<sup>-3</sup>; Nelson et al., 2017), and NH<sub>3(g)</sub> above a maize field in Beltsville, MD USA ranged from 0.6 to 9.6 μg-N m<sup>-3</sup> (average 3.6 ± 2.3 μg-N m<sup>-3</sup>; Meyers et al., 2006). The mean [NH<sub>3(g)</sub>] over Narragansett Bay aligns most closely with the [NH<sub>3(g)</sub>] observed over Tampa Bay (Poor et al., 2001). The flux ranges over Narragansett Bay (this study) have a similar magnitude to other observed fluxes over open water (Table 1). Like [NH<sub>3(g)</sub>], the mean flux of NH<sub>3(g)</sub> over Narragansett Bay aligns most closely with the fluxes over Tampa Bay. To put our measurements into a larger context, the fluxes from this study are small relative to those over a corn canopy that was determined using the REA method during fertilization and other management practices: flux range of  $-8.5 \times 10^{-3}$  to  $8.0 \times 10^{-1}$  μg-N m<sup>-2</sup> s<sup>-1</sup>, with a mean flux of  $3.6 \times 10^{-1}$  μg-N m<sup>-2</sup> s<sup>-1</sup> (Nelson et al., 2017). Our measurements were conducted in a region with no significant agricultural footprint, and a non-agricultural, urban system may be sensitive to these smaller fluxes.

NH<sub>3(g)</sub> concentration was negatively correlated with surface chlorophyll concentration and surface pH measured in the Seekonk River, upstream of the REA system (Figure 6). Past work in this system has shown that chlorophyll concentration responds to inorganic nutrient inputs from rainfall (Balint et al., 2021), suggesting a positive relationship between atmospheric NH<sub>3(g)</sub> concentration and chlorophyll if we assume chlorophyll as a proxy for inorganic nutrient concentration in the water column. Similarly to chlorophyll, pH can be a valuable proxy for

**Table 1**  
*NH<sub>3(g)</sub> Concentration and Direct NH<sub>3(g)</sub> Exchange (Mean and Range) Over Open Water and a Tidal Salt Marsh*

Study location	Mean [NH <sub>3(g)</sub> ] (μg-N m <sup>-3</sup> )	[NH <sub>3(g)</sub> ] range (μg-N m <sup>-3</sup> )	Mean NH <sub>3(g)</sub> flux (μg-N m <sup>-2</sup> s <sup>-1</sup> )	NH <sub>3(g)</sub> flux range (μg-N m <sup>-2</sup> s <sup>-1</sup> )	References
Narragansett Bay, RI	2.1 ± 1.8	0.3 to 8.2	1.2 × 10 <sup>-2</sup>	-2.3 to 6.8 × 10 <sup>-2</sup>	This Work
North Sea Emission, Deposition	0.4 ± 0.4, 0.1 ± 0.1		1.3 × 10 <sup>-3</sup>	-1.2 × 10 <sup>-2</sup> to 7.0 × 10 <sup>-3</sup>	Asman et al. (1994)
Tampa Bay, FL November, July	1.7		1.9 × 10 <sup>-2</sup> , 1.9 × 10 <sup>-3</sup>		Poor et al. (2001)
Chesapeake Bay		0.5 to 7.0			Siefert (2002)
Chesapeake Bay, Baltimore, MD	(NH <sub>3</sub> +NH <sub>4</sub> <sup>+</sup> ) 2.7 ± 1.7		-6.9 × 10 <sup>-4</sup>	-2.3 to 2.7 × 10 <sup>-2</sup>	Larsen et al. (2001)
Chesapeake Bay, Solomons, MD	(NH <sub>3</sub> +NH <sub>4</sub> <sup>+</sup> ) 1.0 ± 0.8		-9.5 × 10 <sup>-4</sup>	-5.2 to 7.0 × 10 <sup>-2</sup>	Larsen et al. (2001)
Tidal Salt Marsh, DE	2.3 ± 1.5, 3.0 ± 0.4		~2.5 × 10 <sup>-4</sup>	~1.1 to 4.8 × 10 <sup>-4</sup>	Lichiheb et al. (2021)

Note. Note that positive flux values are net volatilization; negative flux values are net deposition.

primary production, with higher pH values indicative of greater rates of photosynthesis. However, the inverse relationship observed in this study with both chlorophyll and pH counters the hypothesis that inorganic nutrients are simultaneously increasing atmospheric NH<sub>3</sub> concentration and stimulating primary production. Instead, our results may be reflective of primary production depleting residual inorganic nitrogen. Lag times between nutrient inputs and chlorophyll concentration in this study system remains an area of current research (e.g., Balint et al., 2021; Oviatt et al., 2022), and future work should utilize high temporal resolution water, sediment, and atmospheric flux measurements to further investigate the potential relationship between water column inorganic nitrogen concentration, NH<sub>3(g)</sub> concentration, and NH<sub>3(g)</sub> flux. Co-located deposition and water quality monitoring would provide information on source allocation, trends, risk to sensitive ecosystems, and efficacy of pollution reduction efforts (Amos et al., 2018).

Interestingly, NH<sub>3(g)</sub> flux and concentration were not correlated with environmental variables such as wind speed, wind direction, air temperature, water temperature, or time (from both seasonal and diurnal perspectives) (Table S5 and Figure S3 in Supporting Information S1). However, we note that sampling was conducted under a limited regime, with a need to avoid high wind speed days for safety purposes and the removal of northeastern wind directions from NH<sub>3(g)</sub> flux calculations due to land interference. It is possible that avoiding high wind speed days could bias the data set. Shen et al. (2016) measured NH<sub>3</sub> dry deposition within 1 km of a commercial beef cattle feedlot in Victoria, Australia and estimated that the feedlot accounted for 8.1% of total annual NH<sub>3</sub> emissions. The authors suggest that their lower fraction of emissions deposited locally relative to other feedlot studies (e.g., 16% within 1 km estimated by Hao et al. (2006) and 10.4% within 0.5 km calculated by Walker et al. (2009)) could be attributed to the relatively higher wind speeds at their site. High NH<sub>3</sub> emission rate is favored with high wind speeds; however, windy conditions may also result in quick dispersion and dilution of the NH<sub>3</sub> plume, such that lower NH<sub>3</sub> concentrations and dry deposition are found in downwind regions (Shen et al., 2016). Finally, although future work in this system could utilize a location with less land interference to better resolve the relationship between wind direction and NH<sub>3(g)</sub> flux, we note that such a location (e.g., a piling, buoy, rock outcropping) would be even more vulnerable to sampling during high wind conditions.

We found that the upward flux of NH<sub>3(g)</sub> (i.e., N from the Bay to the atmosphere) dominates during the fall season (Table S6 in Supporting Information S1). Ionized NH<sub>4</sub><sup>+</sup> converts to nonionized NH<sub>3</sub> in alkaline waters (pH above 7.2), which can be lost from the water to the atmosphere as a gas (Vlek and Stumpe (1978)). Vlek and Craswell (1981) concluded that NH<sub>3(g)</sub> volatilization increases with increasing NH<sub>4</sub><sup>+</sup> concentration and water pH. During our fall sampling period, surface water concentrations were high (Figure S4 in Supporting Information S1) and water pH ranged from 7.35 to 7.86.

Loss of N from the Bay to the atmosphere has important implications for urban air quality when considered in the context of seasonal changes in wet atmospheric deposition and surface water NH<sub>3(g)</sub> concentrations. Joyce et al. (2020) found that inorganic N in Providence wet deposition was lowest during the fall season. Adding the wet deposition measurements to our observations, we find that the total (wet + dry) atmospheric deposition of NH<sub>x</sub> is often lower than surface water NH<sub>x</sub> concentrations, which can help to explain the net upward flux. Larsen et al. (2001) estimated the flux of NH<sub>3(g)</sub> into and out of the water at two locations along the Chesapeake Bay (Baltimore (urban) and Solomons (rural), MD), and similarly found that the flux was greatest out of the water during peak surface water concentrations, agreeing with the findings in this study. Like Narragansett Bay, the Chesapeake Bay is a N-limited system that suffers from hypoxic conditions in response to excess N loading in the summer months (Larsen et al., 2001). Interestingly, Walters et al. (2022) observed atmospheric NH<sub>3(g)</sub> in Providence, RI coming from the Narragansett Bay region during the 2018 fall season, further suggesting that surface water may be an important NH<sub>3(g)</sub> source at certain times of the year, although additional studies are needed.

The maximum potential amount of N lost from the Bay to the atmosphere was estimated to be 7,300 mol N d<sup>-1</sup>, using surface water NH<sub>3(g)</sub> concentrations with Henry's Equilibrium. Including this estimate (7,300 mol N d<sup>-1</sup>) into the seasonal fall NH<sub>3(g)</sub> emissions sources for Providence County (US EPA National Emission Inventory), we compute that N released from the Bay to the atmosphere

**Table 2**  
Annual Wet and Dry Atmospheric Deposition for Different N Forms and Total N

	N form	Nixon et al. (1995)	Joyce et al. (2020)
Wet deposition	Nitrate (NO <sub>3</sub> <sup>-</sup> )	9.5	3.1
	Ammonium (NH <sub>4</sub> <sup>+</sup> )	5.6	34.9
	Dissolved Organic Nitrogen (DON)	5.6	11.4
	N form	Nixon et al. (1995)	This Study
Dry deposition	Ammonia (NH <sub>3(g)</sub> )	Not measured	5.9
	Particulate Ammonium (p-NH <sub>4</sub> <sup>+</sup> )	Not measured	0.3
	Nitric Acid (HNO <sub>3(g)</sub> )	5.9	5.9 <sup>a</sup>
	Particulate Nitrate (p-NO <sub>3</sub> <sup>-</sup> )	3.3	3.3 <sup>a</sup>
Total N deposition		<b>29.9</b>	<b>64.8</b>

*Note.* All values are reported in  $\times 10^6$  mol yr<sup>-1</sup>. Annual NO<sub>3</sub><sup>-</sup>, NH<sub>4</sub><sup>+</sup>, NH<sub>3(g)</sub>, p-NH<sub>4</sub><sup>+</sup>, HNO<sub>3(g)</sub>, p-NO<sub>3</sub><sup>-</sup> deposition determined following the Nixon et al. (1995) framework. Dissolved organic nitrogen estimated assuming a 30% contribution to wet total N (e.g., Decina et al., 2018; Kanakidou et al., 2012). The bold values “29.9” and “64.8” reflect total nitrogen deposition (i.e., sum of wet + dry deposition) for Joyce et al. (2020) and Nixon et al. (1995).

<sup>a</sup>HNO<sub>3(g)</sub> and p-NO<sub>3</sub><sup>-</sup> values come from Nixon et al. (1995), as no newer measurements exist for Narragansett Bay.

can make up to ~10% of the total anthropogenic NH<sub>3(g)</sub> emission budget. Using our limited upward flux measurements ( $n = 3$  water-derived), we then calculated the amount of N lost from the Bay to the atmosphere to compare to our estimate. Our observations suggest that 4,200 mol N d<sup>-1</sup> are lost from the Bay to the atmosphere, which is within the same order of magnitude of our other calculated estimate (7,300 mol N d<sup>-1</sup>). Thus, it is likely that N emitted from the Bay can be an important contribution to NH<sub>3(g)</sub> in the atmosphere during the fall season when surface water concentrations are relatively high.

#### 4.2. Estimate of Annual Atmospheric Deposition in Narragansett Bay

In 1989–1990, wet deposition of NO<sub>3</sub><sup>-</sup> and NH<sub>4</sub><sup>+</sup> were monitored, following NADP collection guidelines, in four locations across RI to identify any biases associated with urbanization (Fraher, 1991). An urban-rural gradient was not identified, and therefore Prudence Island (the Southernmost monitoring site located in the center of Narragansett Bay) was selected and considered representative of wet N deposition to the Bay. Dry deposition of total NO<sub>3</sub><sup>-</sup> (HNO<sub>3(g)</sub> and p-NO<sub>3</sub><sup>-</sup>) was also monitored on Prudence Island from 7/90–10/90 using denuders to separate gaseous and particulate phase (Fraher, 1991). Nixon et al. (1995) used these year-round wet (NO<sub>3</sub><sup>-</sup> and NH<sub>4</sub><sup>+</sup>) and seasonal dry (HNO<sub>3(g)</sub> and p-NO<sub>3</sub><sup>-</sup>) deposition observations, along with estimated dissolved inorganic nitrogen (DON), to estimate total annual N deposition to the Bay. DON was estimated following the relationship established by Nowicki and Oviatt (1990), where  $DON = 0.56 \times NO_3^- + 0.49$ . The annual N deposition estimate by Nixon et al., 1995 ( $30.0 \times 10^6$  mol N yr<sup>-1</sup>; Table 2) is currently used for policy driven nutrient budgets for Narragansett Bay, though the total does not include dry deposition of NH<sub>x</sub> since it has not been monitored prior to this study. Based on recent observed wet deposition (NO<sub>3</sub><sup>-</sup> and NH<sub>4</sub><sup>+</sup>; Joyce et al., 2020), estimated DON (Table 2), previous dry deposition of total NO<sub>3</sub><sup>-</sup> (Nixon et al., 1995), and observed dry deposition of NH<sub>x</sub> (this work), we computed a total N deposition to the Bay of  $64.8 \times 10^6$  mol N yr<sup>-1</sup> (Table 2). We note that the updated total N deposition estimate (Table 2) depends on estimated DON and dry deposition of total NO<sub>3</sub><sup>-</sup>, as well as the scalability of our fall NH<sub>x</sub> values to all seasons. We estimated DON by assuming a 30% contribution to wet total N, following recent studies that have shown that DON makes up ~30% of wet N deposition (e.g., Decina et al., 2018; Kanakidou et al., 2012). The DON estimate reported in Nixon et al. (1995) contributes 27% to total wet N, agreeing well with the suggested ~30% contribution. Presumably, the dry deposition of total NO<sub>3</sub><sup>-</sup> would have somewhat changed since 1990. Simulated results from an atmospheric chemistry model (GEOS-Chem) have shown that decreased SO<sub>2</sub> and NO<sub>x</sub> emissions result in more efficient secondary aerosol formation, because aerosol pH and oxidation efficiency increase under those conditions (e.g., Shah et al., 2018). Thus, p-NO<sub>3</sub><sup>-</sup> concentrations in the Northeastern USA have been expected to increase. The seasonal scalability is likely realistic based on year-round NH<sub>3(g)</sub> measurements made by Walters et al. (2022) in the greater Providence area, where observed concentrations averaged  $0.9 \pm 0.5$  μg m<sup>-3</sup>. This average was in good agreement with our

average values for each position (i.e.,  $0.6 \pm 0.4$ ,  $0.8 \pm 0.9$ , and  $0.7 \pm 0.5 \mu\text{g-N m}^{-3}$  for updraft, downdraft, and deadband, respectively). Moreover, Larsen et al. (2001) observed no seasonality in  $\text{NH}_x$  deposition at the urban sampling site along the Chesapeake Bay watershed, nor did they find significant annual differences, suggesting little to no influence of interannual variability in atmospheric conditions. It is interesting to note that the observed atmospheric  $\text{p-NH}_4^+$  was much higher in the city of Providence ( $0.4 \pm 0.3 \mu\text{g-N m}^{-3}$ ; Walters et al., 2022) when compared to over Narragansett Bay ( $0.1 \pm 0.05 \mu\text{g-N m}^{-3}$ ), indicating that the city is more conducive to particulate formation.

#### 4.3. Case Study: 8 August 2020

Elevated  $\text{NH}_x$  concentrations (as high as  $4.3 \mu\text{g-N m}^{-3}$ ) and the largest downward flux of  $\text{NH}_{3(\text{g})}$  ( $-4.6 \times 10^{-1} \mu\text{g-N m}^{-2} \text{s}^{-1}$ ) were observed during the third sampling period in this study, which occurred on 8 August 2020. This day had the warmest air temperatures (between  $0.8$ – $17.1^\circ\text{C}$  warmer than all other sampling days), higher than average wind speeds ( $1.1 \text{ m s}^{-1}$  higher than the average wind speed), and winds originating from the Providence (i.e., urban) region. Thus, it is possible that the meteorological conditions during our third sampling period caused the large downward flux (i.e., N deposited from the atmosphere to the Bay). The higher concentrations observed agree with  $\text{NH}_x$  observations from the city of Providence (e.g.,  $[\text{NH}_x]$  ranged from  $0.3$ – $7.3 \mu\text{g-N m}^{-3}$  in 2018; Walters et al., 2022). However, we note that the scarcity of measurements under these conditions makes it impossible to determine whether this sample is representative of the environment or an artifact of our methodology. Moreover, the wind origin for this sample period was categorized as “indeterminate,” based on the possibility of land interference at the start or end of the runtime. In the future, it would be useful to sample on days with high wind speeds, high temperature, and northeastern wind directions to better understand if these meteorological conditions are conducive to high flux of atmospheric  $\text{NH}_{3(\text{g})}$  to the Bay.

#### 4.4. Sampling Challenges

To our knowledge, this study represents the first attempt to measure  $\text{NH}_{3(\text{g})}$  fluxes between the atmosphere and water directly. The scarcity of  $\text{NH}_{3(\text{g})}$  flux measurements reflects the challenges of the REA sampling technique, and we describe the difficulties encountered in this study as they are important factors to consider for future work over open water.

The REA technique is sensitive to atmospheric disturbance and the position of nearby land features; thus, selecting a sampling location must take these factors into account. The system must be installed in a location with adequate fetch from the prevailing wind direction to avoid land interference. Furthermore, the system must be located on a rigid structure because movement from a floating dock or buoy can influence anemometer measurements. Electrical power from the shore is required to operate the vacuum pump as a gasoline-powered generator would constitute a source of  $\text{NH}_{3(\text{g})}$  emissions. Our REA system was initially installed atop a former shipping wharf on Prudence Island, RI, which provided numerous benefits: the island experiences minimal impact from urban development and has research infrastructure already established on the island by the National Estuarine Research Reserve System; previous dry deposition measurements of  $\text{HNO}_{3(\text{g})}$  and  $\text{p-NO}_3^-$  were conducted by Fraher (1991) on this island; and the wharf placed the system 300 m from shore which allowed flux measurements to be obtained from any wind direction. Unfortunately, the height and size of the wharf caused atmospheric disturbance from southerly wind directions, as evidenced by disproportionate updraft measurements, which ended the use of this location in our study. The system was then moved to a piling in Riverside, RI (located north of Prudence Island) that was accessible during the fall months from a floating dock. While this location did not suffer from the same atmospheric interference as the wharf, its closer proximity to land greatly constrained the wind directions that could be used to measure air-water flux. Furthermore, the use of a floating dock limited access to the sampling tower to the fall months and to when the water height was within 2 hr of high tide, which constrained the number and duration of sampling events that were possible. Lastly, Riverside is substantially more urban than Prudence Island. Nearly 2 million people reside along the watershed, and the majority of these individuals are located on the northern end. In the future, additional measurements along the watershed would be useful to examine heterogeneity in dry deposition of  $\text{NH}_x$  and the flux of  $\text{NH}_{3(\text{g})}$ .

Collecting and quantifying  $\text{NH}_x$  with the temporal resolution necessary for the REA approach also proved challenging. Acid-coated (2% citric acid) honeycomb denuders and a downstream particulate filter (5% citric acid

coated cellulose filter)<sup>23</sup> housed in a ChemComb Speciation Cartridge™ were initially used for the collection of NH<sub>3(g)</sub> and p-NH<sub>4</sub><sup>+</sup> (Koutrakis et al., 1993). This method is susceptible to breakthrough at flow rates greater than 10 L min<sup>-1</sup>, which at ambient NH<sub>x</sub> concentrations necessitated runtimes in excess of 6 hr. The switch to the Riverside, RI location constrained our sampling window to within 2 hr of high tide, which necessitated a switch to filter packs that utilized a higher flow rate (16 L min<sup>-1</sup>) without breakthrough.

## 5. Conclusion

In the first attempt to utilize a relaxed eddy accumulation system over open water, we quantified atmospheric deposition of total ammonia (NH<sub>x</sub> = NH<sub>3(g)</sub> + p-NH<sub>4</sub><sup>+</sup>) to the Narragansett Bay. It is critical to understand these N sources in addressing nutrient pollution management and ecosystem impacts. The quantification of NH<sub>x</sub> deposition and NH<sub>3(g)</sub> flux can vastly improve our understanding of nonpoint source nutrient loading to the coastal ecosystem, allowing for more accurate modeling of biogeochemical and ecological processes. The findings from this study can be used to conduct future dry deposition measurements in other urbanized estuaries.

This study was the first application for determining air-sea fluxes of NH<sub>3(g)</sub> over open water using the REA methodology. Based on a recent separate wet deposition study, total N deposition has doubled in the region since 1990 (Joyce et al., 2020). Including the dry deposition of NH<sub>x</sub> observed in this work to the other available AD observations (wet inorganic N + dry deposition of nitric acid and particulate NO<sub>3</sub><sup>-</sup>) and DON estimate, increases the amount of N entering the Bay from the atmosphere by 9.6%. Under this framework, dry N deposition as a whole makes up 24% of total N deposition for Narragansett Bay. We find that the dominant flux direction for NH<sub>3(g)</sub> is upward during the fall season, which has implications for urban air quality. We also estimate that NH<sub>3(g)</sub> emitted from the Bay to the atmosphere contributes up to 10% of the local NH<sub>3</sub> emission budget. The outcomes of this research can facilitate more informed N pollution management in RI.

## Data Availability Statement

All environmental, concentration, and flux data are available in the Supporting Information S1 and online at: <https://doi.org/10.26300/j604-5d95>.

## References

- Aguilar, C., Fogel, M. L., & Paerl, H. W. (1999). Dynamics of atmospheric combined inorganic nitrogen utilization in the coastal waters off North Carolina. *Marine Ecology Progress Series*, 180, 67–79. <https://doi.org/10.3354/meps180065>
- Amos, H. M., Miniati, C. F., Lynch, J., Compton, J., Templer, P. H., Sprague, L. A., et al. (2018). What goes up must come down: Integrating air and water quality monitoring for nutrients. *Environmental Science & Technology*, 52, 11441–11448. <https://doi.org/10.1021/acs.est.8b03504>
- Asman, W. A. H., Harrison, R. M., & Ottley, C. J. (1994). Estimation of the net air-sea flux of ammonia over the southern bight of the North Sea. *Atmospheric Environment*, 28(22), 3647–3654. [https://doi.org/10.1016/1352-2310\(94\)00192-N](https://doi.org/10.1016/1352-2310(94)00192-N)
- Asman, W. A. H., Sutton, M. A., & Schjørring, J. K. (1998). Ammonia: Emission, atmospheric transport and deposition. *New Phytologist*, 139(1), 27–48. <https://doi.org/10.1046/j.1469-8137.1998.00180.x>
- Balint, S. J., Joyce, E., Pennino, S., Oczkowski, A., McKinney, R., & Hastings, M. G. (2021). Identifying sources and impacts of precipitation-derived nitrogen in Narragansett Bay, RI. *Estuaries and Coasts*, 45(5), 1287–1304. <https://doi.org/10.1007/s12237-021-01029-7>
- Bash, J. O., Cooter, E. J., Dennis, R. L., Walker, J. T., & Pleim, J. E. (2013). Evaluation of a regional air-quality model with bidirectional NH<sub>3</sub> exchange coupled to an agroecosystem model. *Biogeosciences*, 10(3), 1635–1645. <https://doi.org/10.5194/bg-10-1635-2013>
- Benish, S. E., Bash, J. O., Foley, K. M., Appel, K. W., Hogrefe, C., Gilliam, R., & Pouliot, G. (2022). Long-term regional trends of nitrogen and sulfur deposition in the United States from 2002 to 2017. *Atmospheric Chemistry and Physics*, 22(19), 12749–12767. <https://doi.org/10.5194/acp-22-12749-2022>
- Bettez, N. D., & Groffman, P. M. (2013). Nitrogen deposition in and near an urban ecosystem. *Environmental Science & Technology*, 47(11), 6047–6051. <https://doi.org/10.1021/es400664b>
- Bricker, S. B., Longstaff, B., Dennison, W., Jones, A., Boicourt, K., Wicks, C., & Woerner, J. (2008). Effects of nutrient enrichment in the nation's estuaries: A decade of change. *Harmful Algae*, 8(1), 21–32. <https://doi.org/10.1016/j.hal.2008.08.028>
- Businger, J. A., & Oncley, S. P. (1990). Flux measurement with conditional sampling. *Journal of Atmospheric and Oceanic Technology*, 7(2), 349–352. [https://doi.org/10.1175/1520-0426\(1990\)007<0349:FMWCS>2.0.CO;2](https://doi.org/10.1175/1520-0426(1990)007<0349:FMWCS>2.0.CO;2)
- Davidson, E. A., David, M. B., Galloway, J. N., Goodale, C. L., Haeuber, R., Harrison, J. A., et al. (2011). Excess nitrogen in the U.S. environment: Trends, risks, and solutions. *Issues in Ecology*, 15.
- Decina, S. M., Templer, P. H., & Hutrya, L. R. (2018). Atmospheric inputs of nitrogen, carbon, and phosphorus across an urban area: Unaccounted fluxes and canopy influences. *Earth's Future*, 6(2), 134–148. <https://doi.org/10.1002/2017EF000653>
- Decina, S. M., Templer, P. H., Hutrya, L. R., Gatley, C. K., & Rao, P. (2017). Variability, drivers, and effects of atmospheric nitrogen inputs across an urban area: Emerging patterns among human activities, the atmosphere, and soils. *Science of the Total Environment*, 609, 1524–1534. <https://doi.org/10.1016/j.scitotenv.2017.07.166>
- Fenn, M. E., Bytnerowicz, A., Schilling, S. L., Vallano, D. M., Zavaleta, E. S., Weiss, S. B., et al. (2018). On-road emissions of ammonia: An underappreciated source of atmospheric nitrogen deposition. *Science of the Total Environment*, 625, 909–919. <https://doi.org/10.1016/j.scitotenv.2017.12.313>

## Acknowledgments

This work was funded by the Rhode Island Science and Technology Advisory Council (RI-STAC): RIRA-CA-2019. We thank Ruby Ho for analytical support; Kenneth Raposa and Daisy Durant for assistance with site selection and field logistics on Prudence Island, and the Narragansett Bay National Estuarine Research Reserve in Prudence Island, RI and the Squantum Association in Riverside, RI for allowing us to use their properties for data collection.

- Fotiadi, A. K., Lohou, F., Druilhet, A., Serca, D., Said, F., Laville, P., & Brut, A. (2005). Methodological development of the conditional sampling method. Part II: Quality control criteria of relaxed eddy accumulation flux measurements. *Boundary-Layer Meteorology*, *117*(3), 577–603. <https://doi.org/10.1007/s10546-005-4497-x>
- Fowler, D., Sutton, M. A., Flechard, C., & Pitcairn, C. (1997). Ammonia sources, land-atmosphere exchange and effects: A European perspective. In *Proceedings of the workshop on atmospheric nitrogen compounds: Emissions, transport, transformation, deposition and assessment* (pp. 36–46). North Carolina State University.
- Fraher, J. (1991). *Atmospheric wet and dry deposition of fixed nitrogen to Narragansett Bay*. Thesis, University of Rhode Island. University of Rhode Island.
- Fratini, G., & Mauder, M. (2014). Towards a consistent eddy-covariance processing: An intercomparison of EddyPro and TK3. *Atmospheric Measurement Techniques*, *7*, 2273–2281. <https://doi.org/10.5194/amt-7-2273-2014>
- Galloway, J. N., Dentener, F. J., Capone, D. G., Boyer, E. W., Howarth, R. W., Seitzinger, S. P., et al. (2004). Nitrogen cycles: Past, present, and future. *Biogeochemistry*, *70*(2), 153–226. <https://doi.org/10.1007/s10533-004-0370-0>
- Hao, X., Chang, C., Janzen, H. H., Clayton, G., & Hill, B. R. (2006). Sorption of atmospheric ammonia by soil and perennial grass downwind from two large cattle feedlots. *Journal of Environmental Quality*, *35*(5), 1960–1965. <https://doi.org/10.2134/jeq2005.0308>
- Howarth, R. W. (2008). In A. Desbonnet & B. A. Costa-Pierce (Eds.), *Estimating atmospheric nitrogen deposition in the northeastern United States, Springer series: Science for ecosystem based management* (pp. 47–65). Springer-Verlag.
- Jarvi, L. (2009). Turbulent vertical fluxes and air quality measured in urban air in Helsinki. PhD Thesis. University of Helsinki.
- Joyce, E., Walters, W., Le Roy, E., Clark, S., Schiebel, H., & Hastings, M. G. (2020). Highly concentrated nitrogen atmospheric deposition in an urban, coastal region in the United States. *Environmental Research Communications*, *2*(8), 081001. <https://doi.org/10.1088/2515-7620/aba637>
- Kanakidou, M., Duce, R. A., Prospero, J. M., Baker, A. R., Benitez-Nelson, C., Dentener, F. J., et al. (2012). Atmospheric fluxes of organic N and P to the global ocean. *Global Biogeochemical Cycles*, *26*(3), GB3026. <https://doi.org/10.1029/2011GB004277>
- Kljun, N., Calanca, P., Rotach, M. W., & Schmid, H. P. (2004). A simple parameterization for flux footprint predictions. *Boundary-Layer Meteorology*, *112*(3), 503–523. <https://doi.org/10.1023/B:BOUN.0000030653.71031.96>
- Knap, A., Jickells, T., Pszenny, A., & Galloway, J. (1986). Significance of atmospheric-derived fixed nitrogen on productivity of the Sargasso Sea. *Nature*, *320*(6058), 158–160. <https://doi.org/10.1038/320158a0>
- Koutrakis, P., Sioutas, C., Ferguson, S. T., Wolfson, J. M., Mulik, J. D., & Burton, R. M. (1993). Development and evaluation of a glass honeycomb denuder/filter pack system to collect atmospheric gases and particles. *Environmental Science & Technology*, *27*(12), 2497–2501. <https://doi.org/10.1021/es00048a029>
- Larsen, R. K., Steinbacher, J. C., & Baker, J. E. (2001). Ammonia exchange between the atmosphere and the surface waters at two locations in the Chesapeake Bay. *Environmental Science & Technology*, *35*(24), 4731–4738. <https://doi.org/10.1021/es0107551>
- Lehmann, C. M. B., Bowersox, V. C., & Larson, S. M. (2005). Spatial and temporal trends of precipitation chemistry in the United States, 1985–2002. *Environmental Pollution*, *135*(3), 347–361. <https://doi.org/10.1016/j.envpol.2004.11.016>
- Lichiheb, N., Heuer, M., Hicks, B. B., Saylor, R., Vargas, R., Vázquez-Lule, A., et al. (2021). Atmospheric ammonia measurements over a coastal salt marsh ecosystem along the Mid-Atlantic U.S. *Journal of Geophysical Research: Biogeosciences*, *126*(5), e2019JG005522. <https://doi.org/10.1029/2019JG005522>
- LI-COR Biosciences (2021). Eddy covariance processing software (version 7.0). [Software]. LI-COR Biosciences. Retrieved from [www.licor.com/EddyPro](http://www.licor.com/EddyPro)
- Loughner, C. P., Tzortziou, M., Shroder, S., & Pickering, K. E. (2016). Enhanced dry deposition of nitrogen pollution near coastlines: A case study covering the Chesapeake Bay estuary and Atlantic Ocean coastline. *Journal of Geophysical Research*, *121*(23), 221–238. <https://doi.org/10.1002/2016JD025571>
- Meyers, T. P., Luke, W. T., & Meisinger, J. J. (2006). Fluxes of ammonia and sulfate over maize using relaxed eddy accumulation. *Agricultural and Forest Meteorology*, *136*(3–4), 203–213. <https://doi.org/10.1016/j.agrformet.2004.10.005>
- Michaels, A. F., Siegel, D. A., Johnson, R. J., Knap, A. H., & Galloway, J. N. (1993). Episodic inputs of atmospheric nitrogen to the Sargasso Sea: Contributions to new production and phytoplankton blooms. *Global Biogeochemical Cycles*, *7*(2), 339–351. <https://doi.org/10.1029/93GB00178>
- Myles, L., Meyers, T. P., & Robinson, L. (2007). Relaxed eddy accumulation measurements of ammonia, nitric acid, sulfur dioxide and particulate sulfate dry deposition near Tampa, FL, USA. *Environmental Research Letters*, *2*(3), 034004. <https://doi.org/10.1088/1748-9326/2/3/034004>
- Narragansett Bay Commission. (2019). 2019 Phillipsdale surface data. unpublished. Raw data available via the Narragansett Bay commission snapshot of upper Narragansett Bay buoy data export tool. Retrieved from <http://snapshot.narrabay.com/Buoys/Export>
- Narragansett Bay Commission. (2020). 2020 Phillipsdale surface data. unpublished. Raw data available via the Narragansett Bay commission snapshot of upper Narragansett Bay buoy data export tool. Retrieved from <http://snapshot.narrabay.com/Buoys/Export>
- Narragansett Bay Commission. (2021a). 2015–2020 nutrient monitoring. In *Narragansett Bay commission, snapshot of upper Narragansett Bay*. Retrieved from <https://snapshot.narrabay.com/WaterQualityInitiatives/NutrientMonitoring>
- Narragansett Bay Commission. (2021b). 2020 data report. In *Narragansett Bay commission, environmental monitoring and data analysis section*. Retrieved from [https://snapshot.narrabay.com/Services/MossFile.aspx?file=/s/emma/snapshot/Documents/EMDA%20Data%20Reports/2020\\_NBC\\_Annual\\_Data\\_Report.pdf](https://snapshot.narrabay.com/Services/MossFile.aspx?file=/s/emma/snapshot/Documents/EMDA%20Data%20Reports/2020_NBC_Annual_Data_Report.pdf)
- Narragansett Bay Estuary Program. (2017). *State of Narragansett Bay and its watershed*. Technical Report. Chapter 8, Nutrient Loading, pages 166–189.
- National Atmospheric Deposition Program (NADP). (2012). Standard operating procedure for preparation and extraction of URG denuders. SOP Number PR-4074. Revision 1.1.
- National Oceanographic and Atmospheric Administration. (2020). *Sensor specifications and measurement algorithm*. NOAA's Ocean Service Center for Operational Oceanographic Products and Services (CO-OPS). Retrieved from [https://tidesandcurrents.noaa.gov/publications/CO-OPS\\_Measurement\\_Spec.pdf](https://tidesandcurrents.noaa.gov/publications/CO-OPS_Measurement_Spec.pdf)
- Nelson, A. J., Koloutsou-Vakakis, S., Rood, M. J., Myles, L., Lehmann, C., Bernacchi, C., et al. (2017). Season-long ammonia flux measurements above fertilized corn in central Illinois, USA, using relaxed eddy accumulation. *Agricultural and Forest Meteorology*, *239*, 202–212. <https://doi.org/10.1016/j.agrformet.2017.03.010>
- Nixon, S. W., Buckley, B. A., Granger, S. L., Harris, L. A., Oczkowski, A. J., Fulweiler, R. W., & Cole, L. W. (2008). Nitrogen and phosphorus inputs to Narragansett Bay: Past, present, and future. In A. Desbonnet & B. A. Costa-Pierce (Eds.), *Science for ecosystem-based management: Narragansett Bay in the 21st century* (Vol. 101–175). Springer.
- Nixon, S. W., Granger, S. L., & Nowicki, B. L. (1995). An assessment of the annual mass balance of carbon, nitrogen, and phosphorus in Narragansett Bay. *Biogeochemistry*, *31*(1), 15–61. <https://doi.org/10.1007/BF00000805>
- Nowicki, B. L., & Oviatt, C. A. (1990). Are estuaries traps for anthropogenic nutrients? Evidence from estuarine mesocosms. *Marine Ecology Progress Series*, *66*, 131–146. <https://doi.org/10.3354/meps066131>

- Oczkowski, A., Schmidt, C., Santos, E., Miller, K., Hanson, A., Cobb, D., et al. (2018). How the distribution of anthropogenic nitrogen has changed in Narragansett Bay (RI, USA) following major reductions in nutrient loads. *Estuaries and Coasts*, *41*(8), 2260–2276. <https://doi.org/10.1007/s12237-018-0435-2>
- Oviatt, C., Stoffel, H., Huizenga, K., Reed, L., Codiga, D., & Fields, L. (2022). A tale of two spring blooms in a northeast estuary of the USA: How storms impact nutrients, multiple trophic levels and hypoxia. *Hydrobiologia*, *849*(5), 1131–1148. <https://doi.org/10.1007/s10750-021-04768-7>
- Paerl, H. W. (1995). Coastal eutrophication in relation to atmospheric nitrogen deposition: Current perspectives. *Ophelia*, *41*(1), 237–259. <https://doi.org/10.1080/00785236.1995.10422046>
- Poor, N., Pribble, R., & Greening, H. (2001). Direct wet and dry deposition of ammonia, nitric acid, ammonium and nitrate to the Tampa Bay Estuary, FL, USA. *Atmospheric Environment*, *35*(23), 3947–3955. [https://doi.org/10.1016/S1352-2310\(01\)00180-7](https://doi.org/10.1016/S1352-2310(01)00180-7)
- Rao, P., Hutya, L. R., Raciti, S. M., & Templer, P. H. (2014). Atmospheric nitrogen inputs and losses along an urbanization gradient from Boston to Harvard Forest, MA. *Biogeochemistry*, *121*(1), 229–245. <https://doi.org/10.1007/s10533-013-9861-1>
- R Core Team. (2022). *R: A language and environment for statistical computing*. R Foundation for Statistical Computing. Retrieved from <https://www.R-project.org/>
- Redling, K., Elliott, E., Bain, D., & Sherwell, J. (2013). Highway contributions to reactive nitrogen deposition: Tracing the fate of vehicular NO<sub>x</sub> using stable isotopes and plant biomonitors. *Biogeochemistry*, *116*(1–3), 261–274. <https://doi.org/10.1007/s10533-013-9857-x>
- Requia, W. J., Jhun, I., Coull, B. A., & Koutrakis, P. (2019). Climate impact on ambient PM<sub>2.5</sub> elemental concentrations in the United States: A trend analysis over the last 30 years. *Environment International*, *131*, 10488. <https://doi.org/10.1016/j.envint.2019.05.082>
- Rhode Island Geographic Information System (RIGIS) Data Distribution System. (2022). Environmental Data Center, University of Rhode Island, Kingston, Rhode Island. Retrieved from <http://www.rigis.org>
- Schmidt, C. E. (2014). Atmospheric nitrogen deposition: Analysis of a little studied, but important, piece of the N budget in Narragansett Bay, Narragansett Bay national estuarine research Reserve technical reports series 2014:1. Retrieved from <http://nbnerr.org/wp-content/uploads/2017/01/2014-Schmidt-%20NBNERR-Tech-Series-2014.1.pdf>
- Seinfeld, J. H., & Pandis, S. N. (1979). Atmospheric chemistry and physics: From air pollution to climate change. In *A note on the equilibrium relationship between ammonia and nitric acid and particulate ammonium nitrate* (2nd ed.). John Wiley & Sons.
- Shah, V., Jaeglé, L., Thornton, J. A., Lopez-Hilfiker, F. D., Lee, B. H., Schroder, J. C., et al. (2018). Chemical feedbacks weaken the wintertime response of particulate sulfate and nitrate to emissions reductions over the eastern United States. *Proceedings of the National Academy of Sciences*, *115*(32), 8110–8115. <https://doi.org/10.1073/pnas.1803295115>
- Shen, J., Chen, D., Bai, M., Sun, J., Coates, T., Lam, S. K., & Li, Y. (2016). Ammonia deposition in the neighbourhood of an intensive cattle feedlot in Victoria, Australia. *Scientific Reports*, *6*(1), 32793. <https://doi.org/10.1038/srep32793>
- Siefert, R. L. (2002). Assessment of ammonia emissions and deposition from agricultural operations and urban areas in the Chesapeake Bay airshed, final report submitted to EPA (Chesapeake Bay Program), [UMCES technical series No. TS-XX-02CBL].
- U.S. Geological Survey. (2021). National water information system data available on the world wide web (USGS water data for the nation). Retrieved from [https://waterdata.usgs.gov/nwis/inventory?agency\\_code=USGS&site\\_no=01114000](https://waterdata.usgs.gov/nwis/inventory?agency_code=USGS&site_no=01114000)
- Van Damme, M., Clarisse, L., Franco, B., Sutton, M. A., Erisman, J. W., Kruit, R. W., et al. (2020). Global, regional and national trends of atmospheric ammonia derived from a decadal (2008–2018) satellite record. *Environmental Research Letters*, *16*(5), 055017. <https://doi.org/10.1088/1748-9326/abd5e0>
- Vannucci, P. F., & Cohen, R. C. (2022). Decadal trends in the temperature dependence of summertime urban PM<sub>2.5</sub> in the Northeast United States. *ACS Earth Space Chemistry*, *6*(7), 1793–1798. <https://doi.org/10.1021/acsearthspacechem.2c00077>
- Vlek, P. L. G., & Craswell, E. T. (1981). Ammonia volatilization from flooded soils. *Fertilizer Research*, *2*(4), 227–245. <https://doi.org/10.1007/BF01050196>
- Vlek, P. L. G., & Stumpe, J. M. (1978). Effect of solution chemistry and environmental conditions on ammonia volatilization losses from aqueous systems. *Soil Science Society of America Journal*, *42*(3), 416–421. <https://doi.org/10.2136/sssaj1978.03615995004200030008x>
- Walker, J., Spence, P., Kimbrough, S., & Robarge, W. (2009). Inferential model estimates of ammonia dry deposition in the vicinity of a swine production facility. *Atmospheric Environment*, *42*(14), 3407–3418. <https://doi.org/10.1016/j.atmosenv.2007.06.004>
- Walters, W. W., Karod, M., Willcocks, E., Baek, B. H., Blum, D. E., & Hastings, M. G. (2022). Quantifying the importance of vehicle ammonia emissions in an urban area of the Northeastern US utilizing nitrogen isotopes. *Atmospheric Chemistry and Physics*, *22*(20), 13431–13448. <https://doi.org/10.5194/acp-22-13431-2022>
- Xu, L., & Penner, J. E. (2012). Global simulations of nitrate and ammonium aerosols and their radiative effects. *Atmospheric Chemistry and Physics*, *12*(20), 9479–9504. <https://doi.org/10.5194/acp-12-9479-2012>